2021 43rd Annual International Conference of the
IEEE Engineering in Medicine & Biology Society (EMBC)
Oct 31 - Nov 4, 2021. Virtual Conference

Is electric field strength deterministic in cortical neurons' response to transcranial electrical stimulation?

Hyeyeon Chung, Cheolki Im, Hyeon Seo, and Sung Chan Jun

***Abstract*—Transcranial electrical stimulation (tES), which modulates cortical excitability via electric currents, has attracted increasing attention because of its application in treating neurologic and psychiatric disorders. To obtain a better understanding of the brain areas affected and stimulation's cellular effects, a multi-scale model was proposed that combines multi-compartmental neuronal models and a head model. While one multi-scale model of tES that used straight axons reported that the direction of electric field (EF) is a determining factor in a neuronal response, another model of transcranial magnetic stimulation (TMS) that used arborized axons reported that EF magnitude is more crucial than EF direction because of arborized axons' reduced sensitivity to the latter. Our goal was to investigate whether EF magnitude remains a crucial factor in the neuronal response in a multi-scale model of tES into which an arborized axon is integrated. To achieve this goal, we constructed a multi-scale model that integrated three types of neurons and a realistic head model, and then simulated the neuronal response to realistic EF. We found that EF magnitude was correlated with excitation threshold, and thus, it may be one of the determining factors in cortical neurons' response to tES.**

***Clinical Relevance*—This multi-scale model based on biophysical and morphological properties and realistic brain geometry may help elucidate tES's neural mechanisms. Moreover, given its clinical applications, this model may help predict a patient's neuronal response to brain stimulation effectively.**

I. Introduction

Noninvasive brain stimulation (NIBS) has been investigated widely because of its potential to treat neurologic and psychiatric disorders. One of the many ways to apply NIBS is through transcranial electrical stimulation (tES), which modulates cortical neurons' activation by delivering a current directly via electrodes attached to the scalp [1]. Over the past several decades, NIBS has garnered increasing attention because of its application in therapies for neurologic and psychiatric disorders. However, despite the growing numbers of applications, the brain regions affected and cellular mechanisms remain obscure, and thus, researchers have attempted to resolve the uncertainty on a cellular and head level with experiments or computational studies.

With respect to the cellular level, it has been observed that intrinsic neuronal morphology is a pivotal factor in neuronal responses to stimulation [2-4]. Different morphologies cause variations in neuronal responses to stimulation even within a cell type [4]. With respect to the head-model level, researchers have strived to be able to anticipate which regions of the brain will be stimulated. Studies have reported that the brain's anatomy affects the electric field's (EF) spatial distribution and inter-subject variability is a crucial factor in the brain regions implicated [5,6]. Thus, studies have been conducted with a head model, which reflects brain anatomy fully and is obtained from magnetic resonance imaging (MRI), to predict the brain regions affected [5,6]. These two levels of studies imply that the brain's geometry and neurons' morphological and biophysical properties are major determining factors in neuronal responses to stimuli. Thus, to predict neuronal responses precisely, it is imperative to study them at both the brain (macroscopic) and cellular (microscopic) levels.

Attempts have been made to construct a multi-scale model using realistic and multi-compartmental neuron models that are mapped to a realistic head model [7,8]. However, despite these attempts and advances, research on multi-scale modeling is still ongoing because of the technical challenges in combining two scales. Previous research on tES has combined morphologically detailed neurons with a straight axon and head model, and reported a relation between the EF direction and neuronal response [7]. However, a multi-scale study of TMS with a neuron model that consisted of an arborized axon—which is more biologically plausible than is a straight axon—reported that, rather than the direction, EF strength itself may be a determining factor in the neuronal response [8]. In this research, we investigated whether this finding holds true when applied to a multi-scale model of tES consisting of

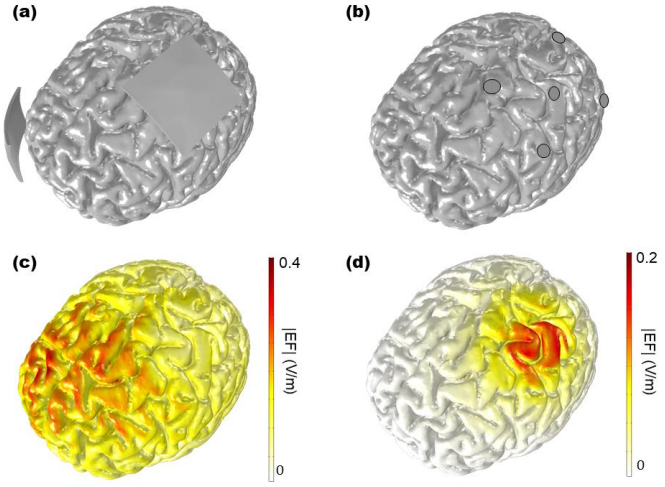

Figure 1. (a)a montage of C-tES, (b)a montage of HD-tES (c)|EF| distribution of C-tES (d) |EF| distribution of HD-tES

*This work was supported by also supported by the Institute of Information & Communications Technology Planning & Evaluation (IITP) grant funded by the Korea government (No. 2017-0-00451) and the '2021 Joint Research Project of Institutes of Science and Technology'.

H. Chung, C. Im, and S. C. Jun are with the School of Electrical Engineering and Computer Science, Gwangju Institute of Science and Technology, Gwangju 61005, South Korea (corresponding author: phone +82-62-715-2216, e-mail: scjun@gist.ac.kr).

H. Seo is with the Medical Device Development Center, Daegu-Gyeongbuk Medical Innovation Foundation, 41061, Daegu, South Korea.

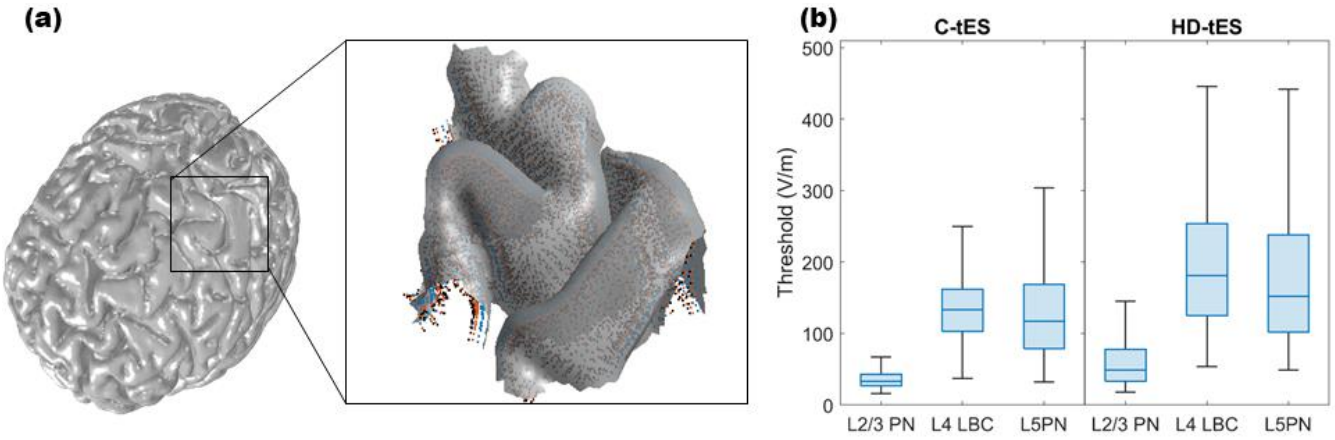

Figure 2. (a) Region of interest, and populated neuron on ROI. Each neuron's soma is represented as a dot. (b) Box plot of excitation threshold for L2/3 PN, L4 LBC, L5 PN stimulated by C- and HD-tES. Outliers are not shown in this figure

arborized axons, to contribute to a better understanding of tES's cellular mechanisms. To achieve this goal, we adopted a multi-compartmental model of a Layer2/3 pyramidal neuron (L2/3 PN), a Layer4 large basket cell (L4 LBC) a Layer5 pyramidal neuron (L5 PN), and that consists of not only realistic dendrites, but also arborized axons. Then, we mapped these neurons to our ROI on a realistic head model based on MRI data to calculate EF. We did so in compliance with conventional-tES (C-tES) and high definition-tES (HD-tES). Thereafter, we simulated neuronal responses while measuring the excitation threshold. As a result, we identified 1) the region C- and HD-tES stimulated, 2) the neurons' excitation threshold, and 3) the correlation between the excitation threshold and EF magnitude.

II. Methods

To develop a multi-scale model for C- and HD-tES, we combined three types of realistic neuron models and realistic EF calculated with a head model, thus this model incurs enormous computational costs. Hence, to achieve cost-effectiveness, we selected a region of interest (ROI) and mapped neurons only in that ROI of the head model. For our ROI, we selected the hand knob area of the precentral gyrus and the area of the postcentral gyrus immediately adjacent to it, where we populated the neuron models (Fig.2a). We calculated C- and HD-tES's realistic EF, as well as that applied to the neuron models in the ROI. We quantified the neuronal response to realistic EF by calculating the excitation threshold, defined as the minimum stimulus amplitude required to cause an action potential in a neuron's soma.

A. Realistic head model and EF

To compute realistic EF, we adopted a realistic volume conduction head model of MRI, which is an exemplar dataset SimNIBS provides [9]. The model consists of five layers (gray matter, white matter, cerebrospinal fluid (CSF), scalp, and skull). We applied two tES montages to this head model: C- and HD-tES. With respect to C-tES, two 5mm × 5 mm patch-type electrodes with a thickness of 2 mm were constructed in the head model, with the active electrode positioned over the ROI and the reference electrode over the right supraorbital region (Fig.1a). For HD-tES, five disc-type electrodes with a 4 mm radius and 1 mm thickness were modeled with one active electrode and four reference electrodes surrounding the active electrode (Fig.1b). The C-tES model did not include gel, but the HD-tES model included CCNY-4, 2 mm-high gels. Then, isotropic electrical conductivity values established previously were assigned to each layer (in S/m): Scalp: 0.465, skull: 0.01, CSF: 1.654, Gray matter: 0.276, white matter: 0.126, patch-type electrode: 1.40, disc-type electrode: 5.8×10^7, gel: 0.30 [10]. More modeling details are described in [7]. Including electrodes, the final tetrahedral mesh of the head model consisted of nearly 2 million nodes and 12.2 million elements. After we constructed the head model's tetrahedral meshes, we computed realistic EF according to the realistic head model for C-and HD-tES by solving the Laplace equation $\nabla\cdot(\sigma\nabla V) = 0$ (V: potential field; σ: electrical conductivity) via the finite element method in COMSOL Multiphysics (v 5.2a, COMSOL, Inc., Burlington, MA, USA).

B. Realistic neuron models

We adopted the multi-compartmental model of a L2/3 PN, L4 LBC, and L5 PN with significantly realistic morphology, all of which are available from ModelDB (Model 241165) [11]. We selected one neuron each from three cell types among the original model's five clones of five cell types, by taking into account pyramidal neurons and basket cells' crucial roles in delivering information in cortical layers. With respect to simulating stimulation of the motor cortex, including L4 LBC, L3 PN, and L5 PN is crucial because PNs process information, and interneurons regulate that processing at the local level [13]. While interneurons are categorized into a variety of cell types according to their morphology and function, basket cells function as intercolumnar inhibitors within their soma's layer [13]. Each neuron model is a series of coupled compartments that consist of segments. A current flow within the neuron model is represented as a voltage difference between each adjacent segment's center points.

C. Multi-scale modeling

To develop a multi-scale model for tES, we coupled the anatomically realistic head and neuronal models. To solve each neuron's EF, we populated neurons in the head model's ROI in the specific layer of the cortex (Fig.2a). Each neuron was aligned according to each face of its tetrahedral elements' center point and the specific layer depth. We assumed an imaginary middle axis to the cell and then aligned the specified axis perpendicular to each of the triangular faces. We took advantage of in vivo experimental results [14] to delineate

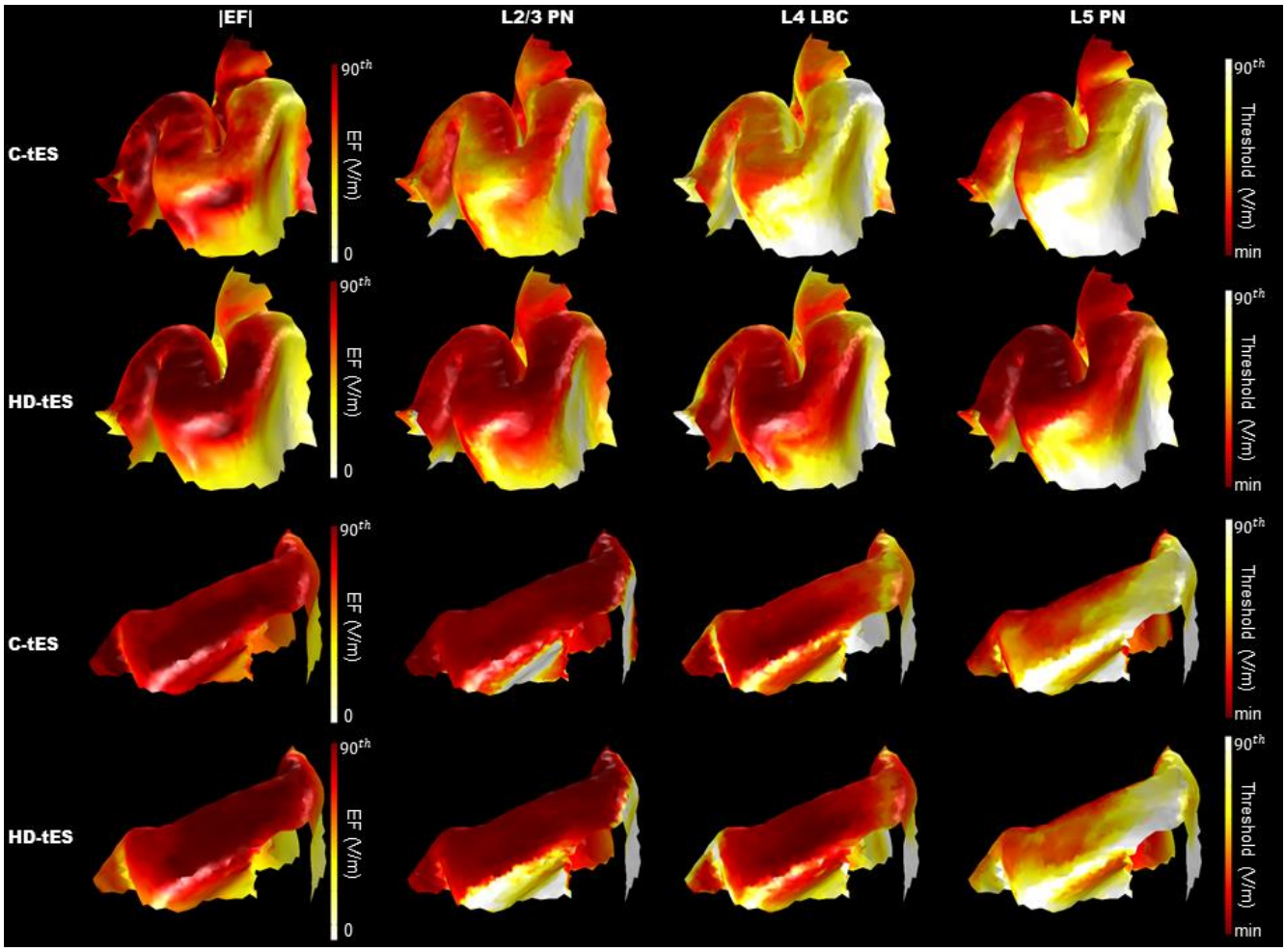

Figure 3. Threshold distribution of L2/3 PN, L4 LBC, L5 PNs by C- and HD-tES in precentral (top two rows) and postcentral gyri (bottom two rows). The threshold was represented as the range from minimal threshold to 90th percentile of the value.

between L4 LBC, L2/3 PN, and L5 PN's cortical layers and soma, which were located in specific layers according to their median depth. Of these three cell types, it is notable that an L5 PN axon stretches from the gray to white matter because of its longer length. In total, 3,132 neurons of each of the three cell types were populated in the ROI aligned to the surface mesh.

We computed the extracellular potential field at each segment's central point for neuron models that populated the hand knob area and a part of the postcentral gyrus based on our simulated realistic EF. We mapped each potential value to each neuron segment's center point via an extracellular mechanism implemented in the NEURON simulation environment (v 7.7) [15] to simulate the neuronal response with a monophasic square waveform. After mapping and simulating this potential field, we obtained an excitation threshold for each populated neuron to quantify the neuronal response to the realistic EF.

III. RESULTS

For C- and HD-tES, we applied a 1 mA stimulus to the targeted ROI for 100 ms via scalp-attached active electrodes. The distribution of simulated EF is depicted in Fig. 3. Our C-tES models displayed more diffuse, but stronger EF, while the EF within our HD-tES was focused, but weaker (Fig.1c,d). C-tES's maximum EF was 0.67 V/m, and HD-tES's was 0.21V/m. This difference between C- and HD-tES was reflected in the neurons' thresholds. Across all three types of neurons, the HD-tES thresholds were higher than those of C-tES (Fig.3) because of its weaker EF in both the pre-and postcentral gyri (Fig.2b). In addition, EF was observed to be focused more on the gyrus's top (crown) and was significantly weaker in magnitude in its bank (deeper regions) for both tESs. This EF distribution was reflected in our three neuron models' threshold distribution. The lowest threshold was found in the crown for both the precentral and postcentral gyri and all three types of neurons, while the highest threshold was found deep in both gyri's sulcal wall (Fig.3). This significant trend was observed across all three types of neurons in both the C- and HD-tES head models, despite differences in the cell localization depth.

Across all tES types, a high threshold area of L4 LBC and L5 PN extended within the sulcal wall, as these two cell types are located at deeper cortical layers than is L2/3 PN, and thus exhibited less EF penetration deep within the gray matter (Fig.3). With respect to the postcentral gyrus, thresholds were higher in the anterior wall than the posterior wall for all cells and tES types (Fig.3), which was consistent with the EF magnitude results. Given the consistency in the EF magnitude and threshold results, we analyzed the correlation between the soma's EF magnitude and each neuron's excitation threshold. We found that the excitation threshold was correlated weakly with the local EF magnitude across all cell types throughout

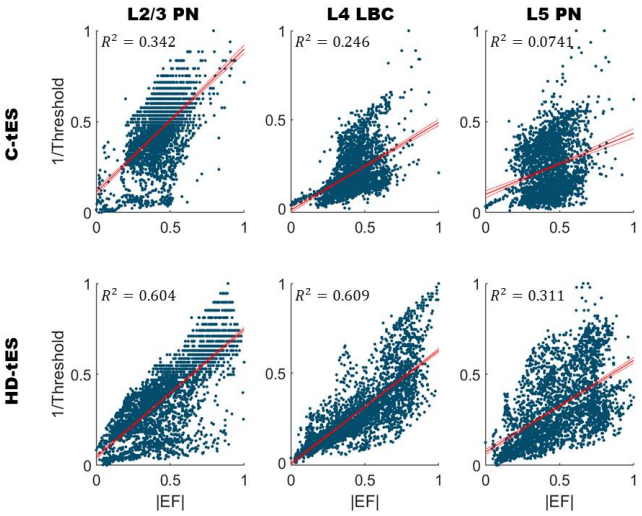

Figure 4. Plot of the inverse threshold against local EF magnitude. Both values are normalized from 0 to 1. The $\boldsymbol{R^2}$ value of each linear regression of the inverse threshold with EF magnitude is included in each figure. Each figure's p-value was significantly smaller than 0.01. 95% confidence intervals are represented as dotted lines around a solid line.

the ROI (Fig.4). The correlation for HD-tES was more pronounced than that for C-tES, possibly because of the HD-tES's focality. However, in the case of L5 PN stimulated by C-tES, the threshold was not correlated significantly with EF magnitude ($R^2 < 0.1$).

IV. DISCUSSION

A prior simulation study of TMS with a neuron model comprised of arborized axons reported that EF strength itself is a crucial factor in a neuronal response [8]. In contrast, a previous study on the simulation of tES with realistic neurons that consisted of a straight axon reported that the relative direction of EF influenced cortical neurons' response notably [7]. These conflicting results may be attributable to arborized axons' reduced sensitivity to EF direction [4]. However, arborized axons are more biologically plausible, hence, their simulation is more realistic. Considering previous studies and their biological plausibility [7,8], our goal was to identify whether EF strength itself is a determining factor in cortical neurons' response in both C and HD-tES when the neuron models consisted of arborized axons.

The realistic EF based on a realistic head model and uniform EF, which was calculated from a cube rather than a head model and excluded spatial information of each neuron, displayed a significant difference in excitation thresholds. Concerning uniform EF, the threshold of L4 LBC was lower than others and the threshold of L3 and L5 PN were similar to each other. However, in the case of realistic EF based on a head model, the threshold of L3 PN was much less than other neurons (Fig.2b). This is attributable to the difference in the specific cortical layer in which a cell is located, in that L5 PN is located deeper than is L4 LBC, which in turn is found deeper than is L3 PN. Based on this, we can infer that EF distribution is a more crucial factor in a neuronal response than a neuron's intrinsic biophysical property, such as its intrinsic threshold.

We observed a low threshold on the gyral crown and a high threshold deep in the sulcal wall, which was consistent with the regions of strong and weak EF. Given this consistency, we analyzed the relation between local EF magnitudes and thresholds, and found that the excitation threshold overall was related to EF magnitude. However, in the case of L5 PN, the thresholds were correlated significantly less than other cell types for both C- and HD-tES. This may be because the L5 PN axon penetrates the white matter, which EF scarcely reaches. With the exception of the case of L5 PN stimulated by C-tES, the thresholds were correlated with local EF magnitude, but not to the same extent as in [8]. This discrepancy may be attributable to the difference in the method chosen to apply NIBS: tES or TMS. Regardless, a previous tES study reported that radial EF, rather than EF magnitude, was the determining factor in cortical neurons' activation, which neither of our results supported [7]. Given our results and the controversy about whether the major factor in cortical activation is EF magnitude or radial EF, it is clear that further studies that investigate the relationship between threshold and radial EF using realistically arborized neuron models are imperative.

REFERENCES

[1] A. V. Peterchev, et al, "Fundamentals of transcranial electric and magnetic stimulation dose: Definition, selection, and reporting practices," *Brain Stimulation*, vol. 5, no. 4, pp. 435–453, 2012.

[2] G.-S. Yi, J. Wang, B. Deng, and X.-L. Wei, "Morphology controls how hippocampal CA1 pyramidal neuron responds to uniform electric fields: a biophysical modeling study," *Scientific Reports*, vol. 7, no. 1, 2017.

[3] T. Radman, R. L. Ramos, J. C. Brumberg, and M. Bikson, "Role of cortical cell type and morphology in subthreshold and suprathreshold uniform electric field stimulation in vitro," *Brain Stimulation*, vol. 2, no. 4, 2009.

[4] A. S. Aberra, A. V. Peterchev, and W. M. Grill, "Biophysically realistic neuron models for simulation of cortical stimulation," *Journal of Neural Engineering*, vol. 15, no. 6, p. 066023, 2018.

[5] A. Opitz, W. Paulus, S. Will, A. Antunes, and A. Thielscher, "Determinants of the electric field during transcranial direct current stimulation," *NeuroImage*, vol. 109, pp. 140–150, 2015.

[6] I. Laakso, M. Mikkonen, S. Koyama, A. Hirata, and S. Tanaka, "Can electric fields explain inter-individual variability in transcranial direct current stimulation of the motor cortex?," *Scientific Reports*, vol. 9, no. 1, 2019.

[7] H. Seo and S. C. Jun, "Relation between the electric field and activation of cortical neurons in transcranial electrical stimulation," *Brain Stimulation*, vol. 12, no. 2, pp. 275–289, 2019.

[8] A. S. Aberra, B. Wang, W. M. Grill, and A. V. Peterchev, "Simulation of transcranial magnetic stimulation in head model with morphologically-realistic cortical neurons," *Brain Stimulation*, vol. 13, no. 1, pp. 175–189, 2020.

[9] A. Thielscher, A. Antunes, and G. B. Saturnino, "Field modeling for transcranial magnetic stimulation: A useful tool to understand the physiological effects of TMS?," *37th IEEE Int. Conf. EMBC,* 2015.

[10] A. Thielscher, A. Opitz, and M. Windhoff, "Impact of the gyral geometry on the electric field induced by transcranial magnetic stimulation," *NeuroImage*, vol. 54, no. 1, pp. 234–243, 2011.

[11] A. S. Aberra, A. V. Peterchev, and W. M. Grill, "Biophysically Realistic models for simulation of cortical stimulation. ModelDB 2018. https://senselab.med.yale

[12] H. Markram, et al., "Reconstruction and simulation of neocortical microcircuitry," Cell, vol.163, no.2, pp456-492, 2015.

[13] G. M. Shepherd and S. Grillner, in *Handbook of brain microcircuits*, 2nd ed., Oxford, NY: Oxford university press, 2018, pp. 67–74.

[14] DeFelipe, J., Alonso-Nanclares, L. & Arellano, J.I. "Microstructure of the neocortex: Comparative aspects," *J Neurocytol, vol.* 31**,** 2002, pp**.**299–316

[15] M. L. Hines and N. T. Carnevale, "The NEURON Simulation Environment," *Neural Computation*, vol. 9, no. 6, pp. 1179–1209, 1997.